Evaluation of the LandscapeDNDC model for drained peatland forest management, LDNDC v 1.35.2 (revision 11434)

Ahmed Shahriyer[1], David Kraus[2], Tiina Markkanen[1], Mika Korkiakoski[1], Helena Rautakoski[1], Suvi Orttenvuori[1], Yao Gao[3], Henri Kajasilta[1], Rüdiger Grote[2], Annalea Lohila[1,4], and Tuula Aalto[1]

[1]Climate System Research, Finnish Meteorological Institute, Helsinki, Finland
[2]Institute of Meteorology and Climate Research Atmospheric Environmental Research (IMKIFU), Karlsruhe Institute of Technology, Garmisch-Partenkirchen, Germany
[3]Department of Civil Engineering, University of Hongkong, Hongkong, China
[4]Institute for Atmospheric and Earth System Research/Physics (INAR), Faculty of Science, P.O. Box 68, 00014 University of Helsinki, Helsinki, Finland

Correspondence: Ahmed Shahriyer (ahmed.hasan.shahriyer@fmi.fi)

1 supplementary material

1.1 Leaf area index

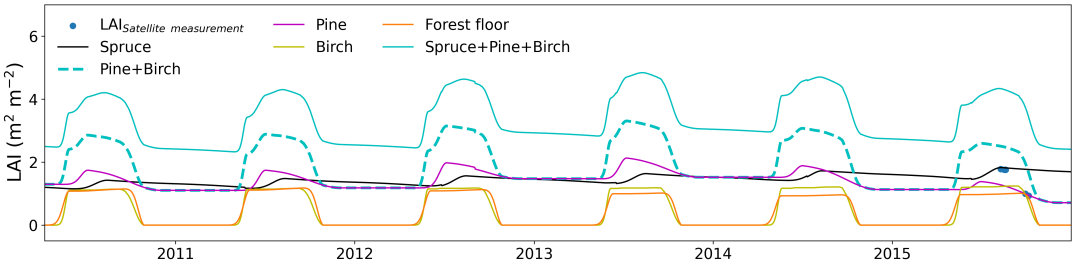

Figure S1. Individual species one-sided modeled Leaf Area Index (LAI) before harvest along with Spruce+Pine+Birch in cyan and pine+Birch in cyan dashed line.

1.2 Water table

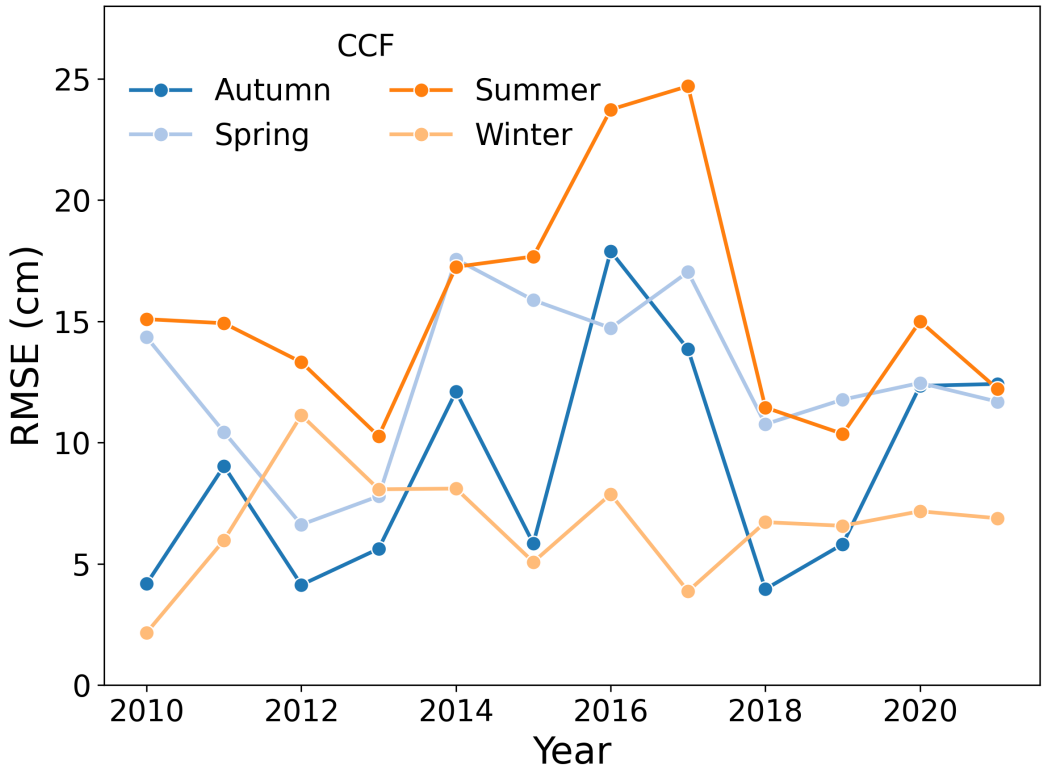

Figure S2. Water table Root Mean Square Error between model and observations at the CCF stand at different seasons.

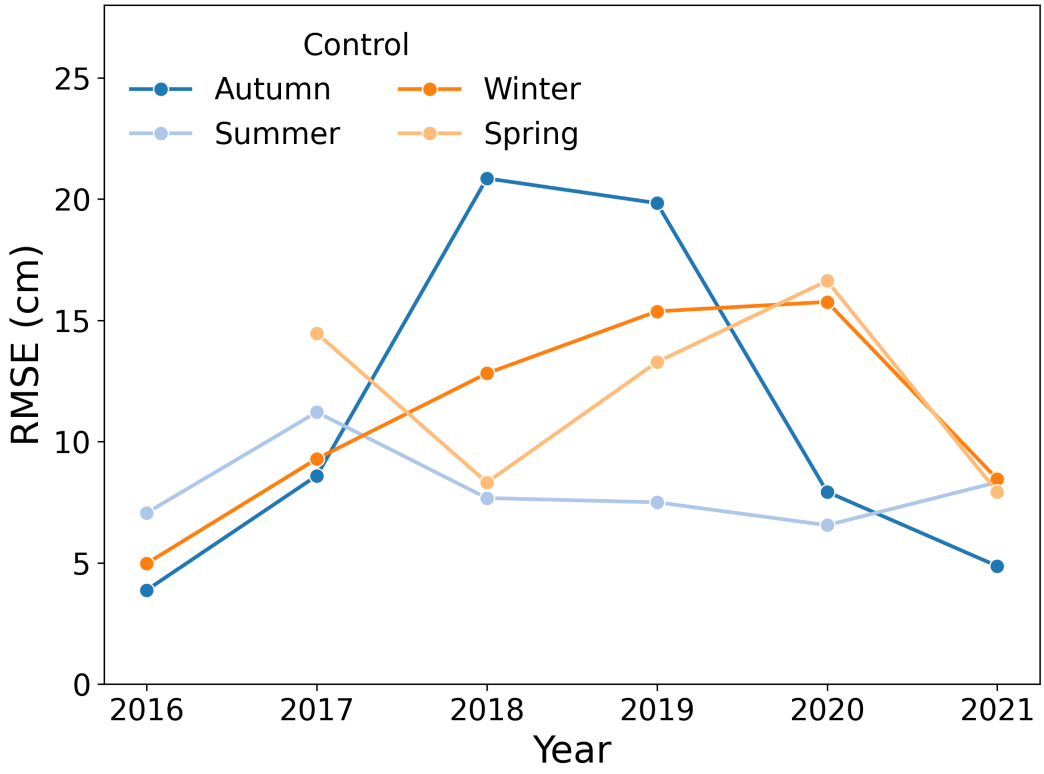

Figure S3. Water table Root Mean Square Error between model and observations at the CCF stand at different seasons.

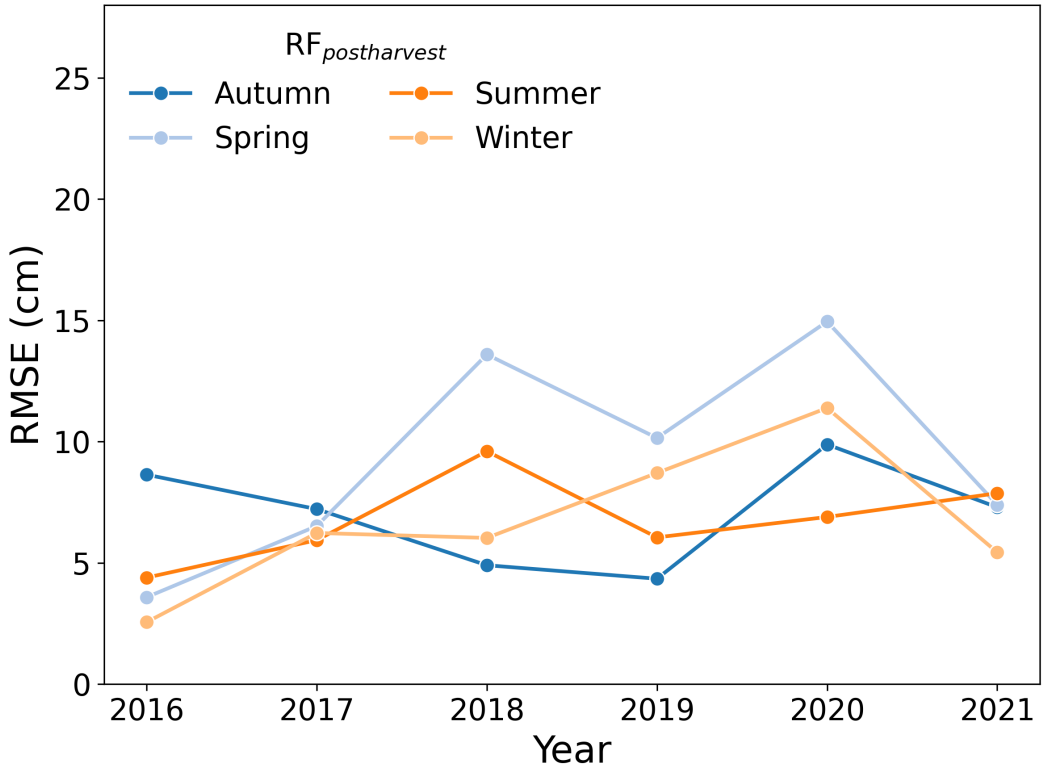

Figure S4. Water table Root Mean Square Error between model and observations at the CCF stand at different seasons.

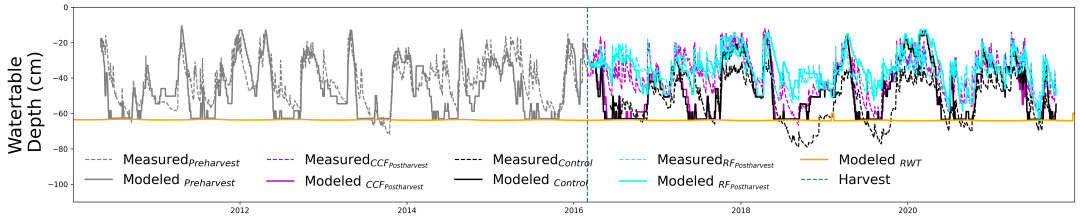

Figure S5. Modeled (solid) and measured (dashed) water table at pre-harvest (gray), Control (black), CCF$_{postharvest}$ (magenta), RF$_{postharvest}$ (cyan) conditions. Additionally the reference water table (RWT) shown in orange and vertical dashed line shows the time of harvest

1.3 Dynamics of CO_2 exchange before and after harvest

NEE$_{mod}$ was better after calibrating the WT than the NEE estimated from the simulation with RWT. The calibrated NEE$_{mod}$ was similar in magnitude and temporal dynamics as NEE$_{EC}$ with some minor discrepancies in pre-harvest condition (Fig. S 10a). Highest RMSE 9.5 $g\ CO_2\ m^{-2}\ d^{-1}$ in the NEE was in the summer 2010 between model and observations (Fig S 11). High spring, summer and autumn RMSE values were also observed in 2014 compared to other years. Model is simulating

similar seasonality for GPP and TER compared to EC based estimates (Fig. S 10b and 10c, respectively). Highest discrepancy was observed in summer 2014 for GPP_{mod} (RMSE 17.1 $g\ CO_2\ m^{-2}\ d^{-1}$ Fig S 11). Model captured the TER well other than the high respiration peaks in the summer of 2010 and 2013. The model was also producing slightly higher winter respiration compared to what was estimated from observations in the beginning of 2013 (Fig. S 10c). Highest RMSE in TER_{mod} was observed in summer of 2010 and 2014 (Fig S 11).

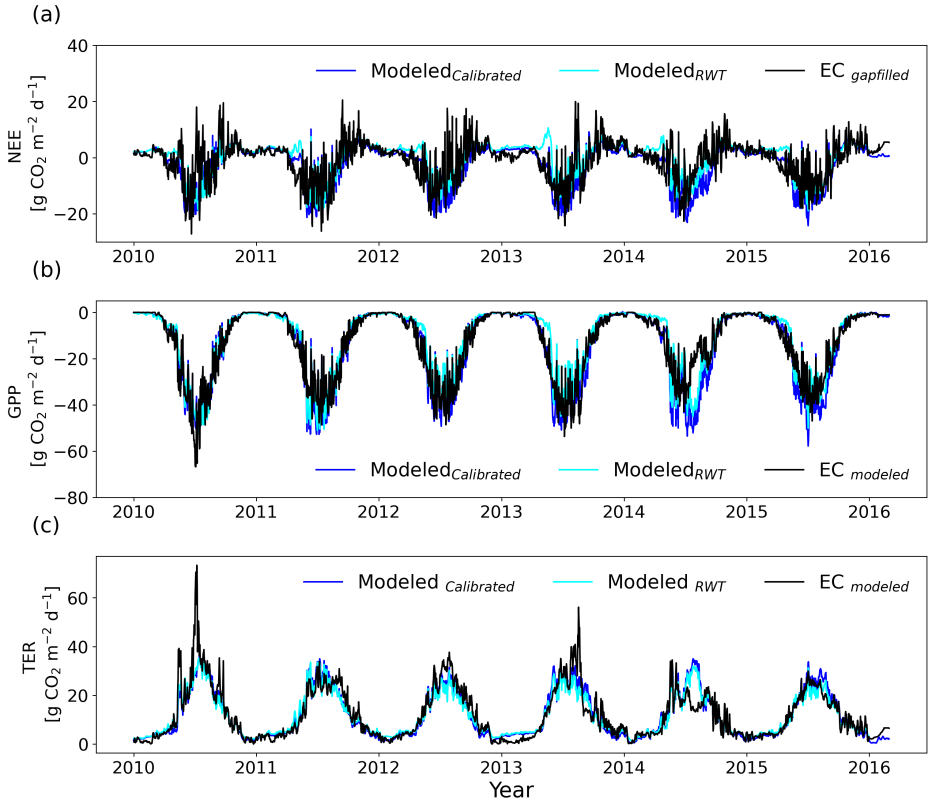

Figure S6. Daily sum of **(a)** NEE, **(b)** GPP and **(c)** TER for mature forest at pre-harvest conditions. Cyan and black lines indicate the modeled CO_2 flux at reference water table (RWT) and calibrated water table, respectively. EC-based estimates of CO_2 flux are shown in blue. Negative values indicate uptake by the ecosystem, and positive values indicate the emission of CO_2 into the atmosphere.

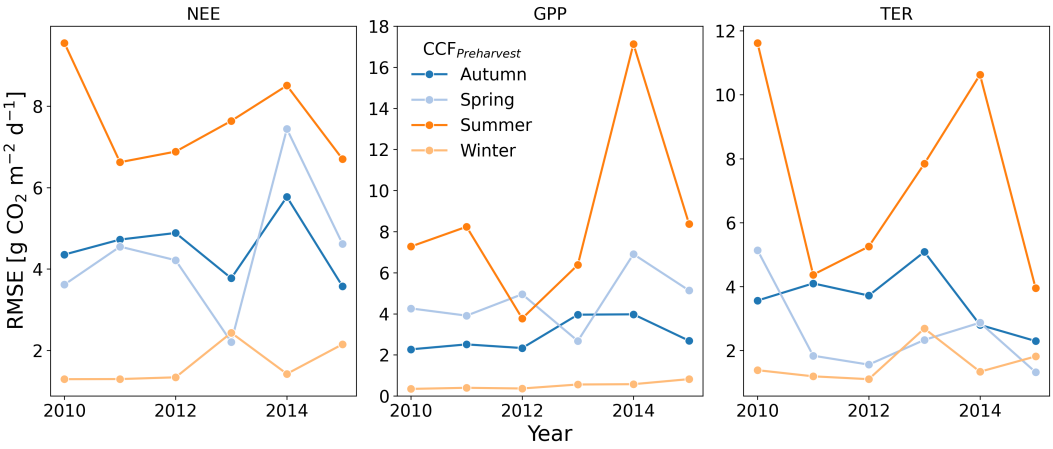

Figure S7. Seasonal Root Mean Square Error (RMSE) of NEE between Model and observations at pre-harvest conditions.

After the selective harvest in 2016, NEE was simulated well for 2017, 2020 and 2021. To an extent, this was also true for late summer and autumn 2018 and 2019, except that the model produced higher uptake (NEE) in spring and early summer for those years (Fig. S 12a). 2016 summer and autumn had noticeable deviation in NEE, while GPP was overestimated by the model and TER was underestimated (Fig S 12b and c, respectively). In spring and early summer 2018 and 2019, GPP and TER were overestimated by the model. Summer RMSE for NEE varied around $6-8\ g\ CO_2\ m^{-2}\ d^{-1}$ and other seasons it was lower than $6\ g\ CO_2\ m^{-2}\ d^{-1}$ and most of the time it was lower than $4\ g\ CO_2\ m^{-2}\ d^{-1}$ (Fig. S 13). Highest RMSE in GPP was observed in 2018 summer and in TER it was 2019 summer.

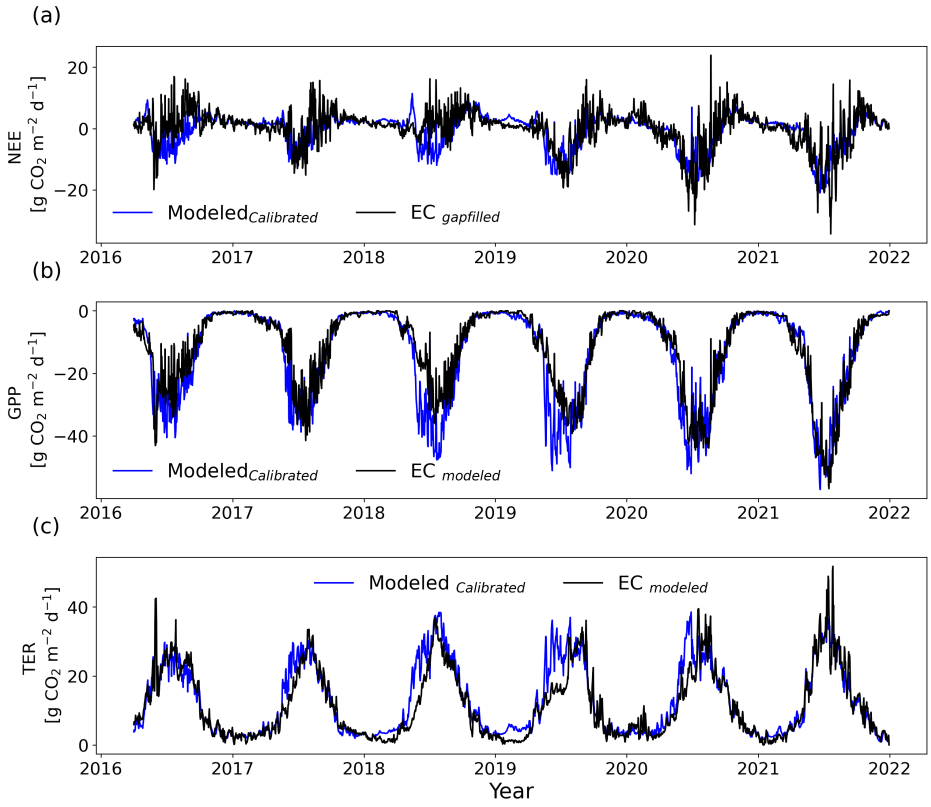

Figure S8. Daily sum of **(a)** NEE , **(b)** GPP and **(c)** TER at post-harvest conditions in continuous cover forestry ($CCF_{postharvest}$) stand. Blue and black lines indicate the modeled and EC-based estimates, respectively. Negative values indicate uptake by the ecosystem, and positive values indicate the emission of CO_2 into the atmosphere.

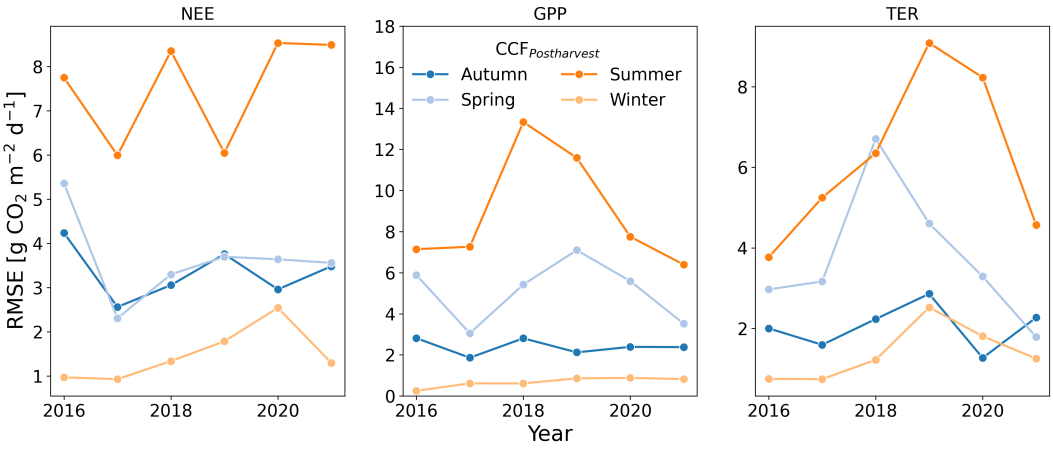

Figure S9. Seasonal Root Mean Square Error (RMSE) of NEE between Model and observations at $CCF_{postharvest}$ conditions.

NEE simulations after clear-cut captured the gradual transition from higher daily net source during the first three years after harvest to lower daily net source or sometimes even sink in the next three years during the summer season (Fig. S 14a). Simulated NEE had the best agreement with measurements 2019-2021 and, to an extent, Autumn 2018. NEE from May-August in 2016 and 2017 were underestimated by the model and indicated ecosystem being a smaller source of CO_2 compared to the measurement. The GPP_{mod} was similar to the GPP_{EC} for 2016–2019, while the GPP for late spring and early summer 2020 and 2021 was slightly overestimated by the model (Fig. S 14b). TER_{mod} was underestimated compared to the TER_{EC} for the summers of 2016 and 2017 and overestimated for late springs and early summers of 2020 and 2021. 2018 and 2019 TER was represented by the model (Fig. S 14c).

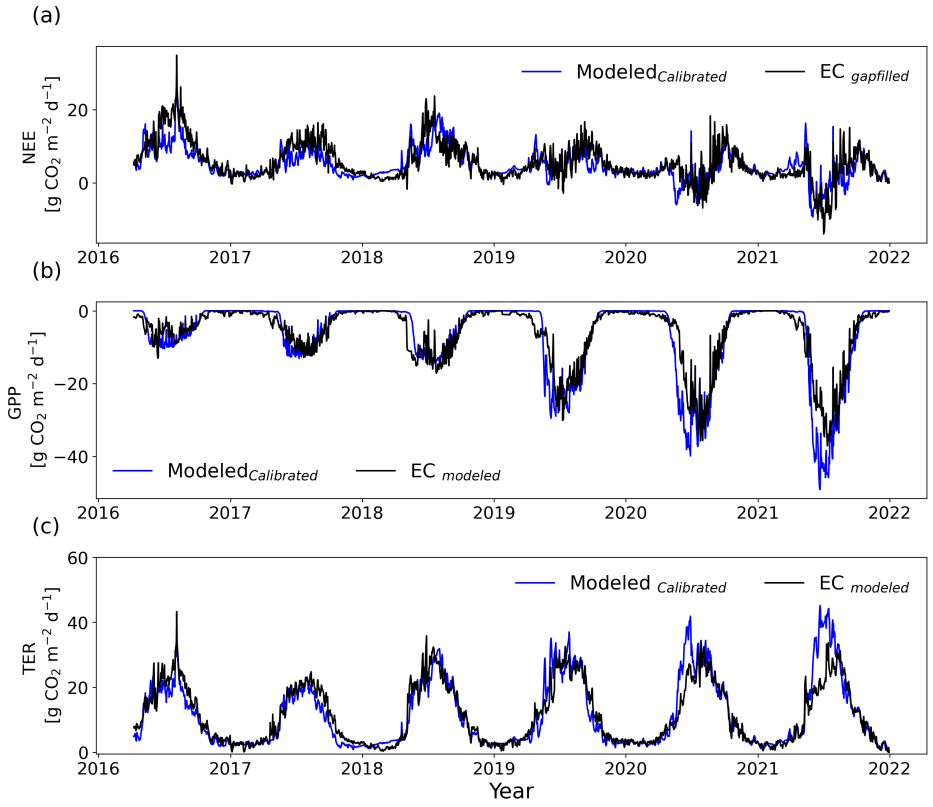

Figure S10. Daily sum of **(a)** NEE, **(b)** GPP and **(c)** TER at post-harvest conditions in rotational forestry ($RF_{postharvest}$) stand. Blue and black lines indicate the modeled and EC-based estimates, respectively. Negative values indicate uptake by the ecosystem, and positive values indicate the emission of CO_2 into the atmosphere.

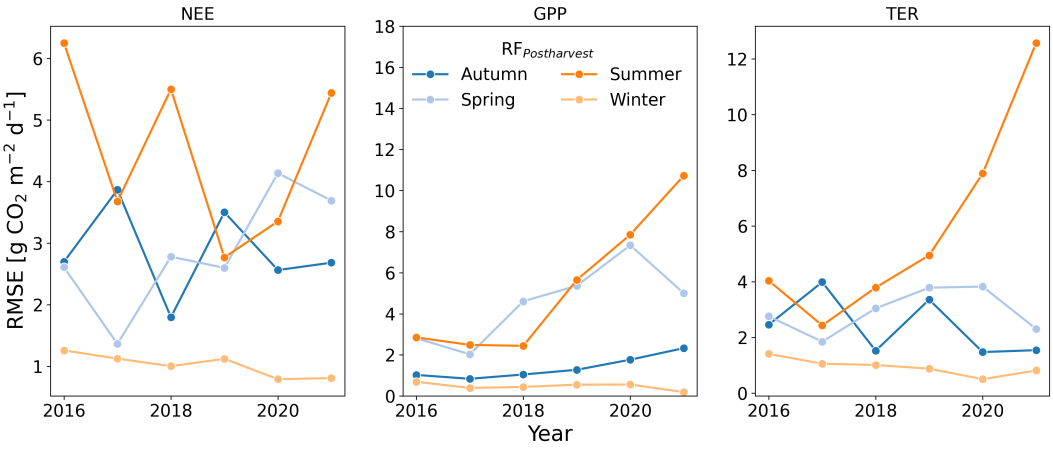

Figure S11. Seasonal Root Mean Square Error (RMSE) of NEE between Model and observations at RF$_{postharvest}$ conditions.

For half-hourly data, r between NEE$_{mod}$ and NEE$_{EC}$ were 0.82, 0.72 and 0.79 for pre-harvest, CCF$_{postharvest}$ and RF$_{postharvest}$, respectively. NSE for NEE of the pre-harvest, CCF$_{postharvest}$ and RF$_{postharvest}$ varied from 0.66, 0.49 and 0.57, respectively (Fig. S 16 a,b and c). For GPP, r was between 0.93-0.94 while NSE was between 0.69-0.84 (Fig. S 16 d,e and f). For TER, r was between 0.88-0.92 and NSE was between 0.75-0.81 (Fig. S 16 g,h and i).

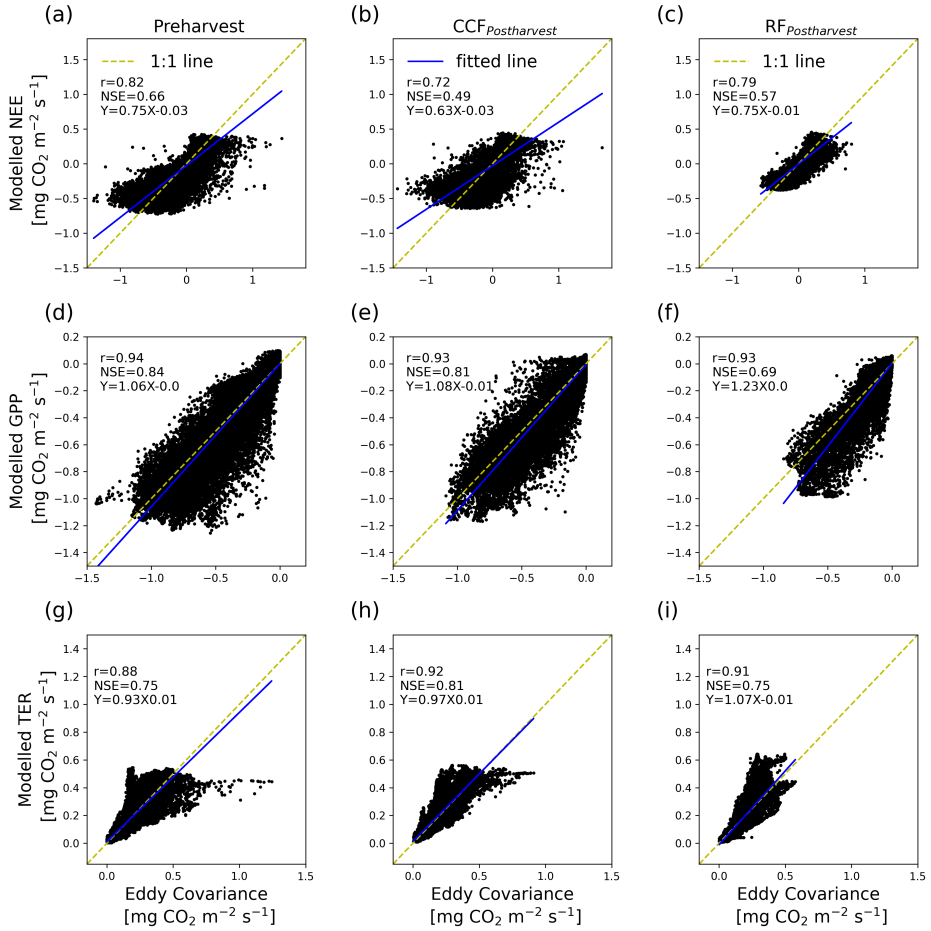

Figure S12. Half hour model and observation comparison for NEE (a,b,c), GPP (d,e,f) and TER (g,h,i) of pre-harvest, CCF$_{postharvest}$ and RF$_{postharvest}$ conditions. Correlation coefficients (r) and Nash-Sutcliff model efficiency (NSE) are given in the figures. Yellow dashed lines and blue lines are the 1:1 lines and fitted lines. The equations for fitted lines are given as Y.